

# Geophysical Research Letters

## RESEARCH LETTER

10.1029/2019GL085997

### Key Points:

- A ~200- $\mu\text{m}$ -sized melt inclusion-bearing zircon fragment was found in lunar feldspathic breccia meteorite NWA 10049
- Melt inclusions in this zircon are compositionally consistent with lunar immiscible silica-rich melts
- The zircon is 4.38 Ga and provides microscale evidence for ancient immiscible silica-rich melt on the Moon

### Supporting Information:

- Supporting Information S1

### Correspondence to:

S. Li and J. Liu,  
lishijiepsc@mail.gyig.ac.cn;  
liujianzhong@mail.gyig.ac.cn

### Citation:

Zeng, X., Joy, K. H., Li, S., Lin, Y., Wang, N., Li, X., et al. (2020). Oldest immiscible silica-rich melt on the Moon recorded in a ~4.38 Ga zircon. *Geophysical Research Letters*, 47, e2019GL085997. <https://doi.org/10.1029/2019GL085997>

Received 27 OCT 2019

Accepted 5 FEB 2020

Accepted article online 7 FEB 2020

## Oldest Immiscible Silica-rich Melt on the Moon Recorded in a ~4.38 Ga Zircon

Xiaoja Zeng<sup>1,5</sup> , Katherine H. Joy<sup>3</sup> , Shijie Li<sup>1,2</sup>, Yangting Lin<sup>4</sup>, Nian Wang<sup>4</sup>, Xiongyao Li<sup>1,2,5</sup>, Yang Li<sup>1,2,5</sup>, Jialong Hao<sup>4</sup>, Jianzhong Liu<sup>1,2</sup> , and Shijie Wang<sup>6</sup>

<sup>1</sup>Center for Lunar and Planetary Sciences, Institute of Geochemistry, Chinese Academy of Sciences, Guiyang, China, <sup>2</sup>CAS Center for Excellence in Comparative Planetology, Hefei, China, <sup>3</sup>Department of Earth and Environmental Sciences, University of Manchester, Manchester, UK, <sup>4</sup>Key Laboratory of Earth and Planetary Physics, Institute of Geology and Geophysics, Chinese Academy of Sciences, Beijing, China, <sup>5</sup>Key Laboratory of Space Manufacturing Technology, Chinese Academy of Sciences, Beijing, China, <sup>6</sup>State Key Laboratory of Environmental Geochemistry, Institute of Geochemistry, Chinese Academy of Sciences, Guiyang, China

**Abstract** The temporal duration of lunar-evolved magmatism is still poorly constrained. In lunar meteorite Northwest Africa (NWA) 10049, a melt inclusion-bearing zircon fragment provides a new tool to understand the composition and age of the melts from which zircon directly crystallized. The studied zircon-hosted melt inclusions are silica rich and iron poor (e.g., ~80–90 wt% SiO<sub>2</sub>; <0.5 wt% FeO), compositionally similar with immiscible silica-rich melts found in Apollo rocks. Nano-SIMS U–Pb analyses of the zircon yielded a minimum crystallization age of 4,382 ± 40 Ma, older than the ages for Apollo highly evolved alkali suite lithologies (~3.8–4.33 Ga). Our study shows that the melt inclusion-bearing zircon in NWA 10049 is the oldest microscale evidence for documenting immiscible silica-rich melts in lunar samples, suggesting that lunar-evolved silica-rich melts were prevalent as early as ~4.38 Ga. This work implies that there would be a prolonged silicic magmatism occurred on the Moon.

**Plain Language Summary** Lunar-evolved silica-rich melt is thought to be related to the formation of highly silicic lithologies (e.g., granitic lithologies). These rock types have been observed in Apollo returned samples as lithic clasts and also have been detected by remote-sensing data as silicic domes. The Apollo-evolved lithologies give a wide range of crystallization ages from ~3.8–4.33 Ga. However, there is still unclear about the temporal duration of lunar-evolved magmatism and volcanism. In lunar meteorite breccia NWA 10049, a melt inclusions-bearing zircon fragment provides a new tool to understand the composition and age of the melts from which zircon directly crystallized. The studied zircon-hosted melt inclusions are compositionally similar with immiscible silica-rich melts found in Apollo rocks. Nano-SIMS U–Pb analyses of the zircon yielded a minimum crystallization age of ~4.38 Ga. This age is older than the ages for Apollo-returned granites (up to 4.33 Ga) and ancient basaltic volcanism (i.e., up to ~4.37 Ga), making the studied zircon is the oldest microscale evidence for documenting lunar silicate liquid immiscibility.

## 1. Introduction

Highly silicic-evolved lithologies (e.g., granite and felsite) are rare on the Moon. They were first recognized as small fragments in Apollo samples (e.g., Jolliff, 1991; Jolliff et al., 1999; Taylor et al., 1980; Warner et al., 1978; Seddio et al., 2013) and were followed by the discovery of silica-rich “evolved” clasts in a wide range of lunar meteorites (e.g., Northwest Africa [NWA] 773, NWA 4472, and Sau 169; Fagan et al., 2014; Joy et al., 2011; Lin et al., 2012). U–Pb analysis of zircon for Apollo silicic lithologies yields crystallization ages ranging from 3.88 to 4.33 Ga (e.g., Grange et al., 2009; Hinton & Meyer, 1991; Meyer et al., 1996; Thiessen et al., 2018; Zhang et al., 2012).

Magma differentiation with silicate liquid immiscibility (SLI) is thought to be one of the mechanisms to account for chemical unmixing in terrestrial ferrobasalt sequences (Charlier et al., 2011; Jakobsen et al., 2005; Roedder, 1979) and the formation of lunar highly silicic lithologies (Gullikson et al., 2016; Hess, 1989; Jolliff, 1991; Roedder & Weiblen, 1970; Rutherford et al., 1976). These studies suggest that silica-rich rocks are formed as the result of extensive crystal fractionation (90–98%) of basaltic magma, as the

© 2020. The Authors.

This is an open access article under the terms of the Creative Commons Attribution License, which permits use, distribution and reproduction in any medium, provided the original work is properly cited.

residual melt chemically evolves and segregates into a Si-K-rich (felsic) and Fe-rich (Fe-basaltic) melts (Hess, 1989; Roedder & Weiben, 1970) during anhydrous, low-pressure fractional crystallization (Charlier & Grove, 2012). Evidence for liquid immiscibility on the Moon is commonly documented in melt inclusions (MIs) of silicates (e.g., plagioclase) that crystallized from basaltic magmas (Roedder, 1984; Snyder et al., 1993; Shearer et al., 2001). In addition, it has been proposed that silicate liquid immiscibility was important during the last stages of lunar magma ocean crystallization and was responsible for producing post-lunar magma ocean granites and felsites that are part of the alkali suite (Jolliff, 1991; Neal & Taylor, 1989; Taylor et al., 1980).

Zircon ( $\text{ZrSiO}_4$ ) is a common accessory mineral in lunar samples, providing a useful chronological tool to place time constraints on the magmatism throughout lunar history (e.g., Hinton & Meyer, 1991; Mattinson et al., 1996; Merle et al., 2017; Meyer et al., 1996; Nemchin et al., 2009, 2012). MIs in old zircon can provide an unambiguous method to directly determine compositions of melts from which zircon crystallized and possibly reveal the magma evolution history (e.g., Thomas et al., 2003). Recently, a zircon fragment from lunar feldspathic breccia meteorite NWA 10049 has been observed to contain three silica-rich rhyolitic MIs. This MI-bearing zircon provides an opportunity to reveal the timing of chemically evolved melts on the Moon. This work aims to investigate the crystallization age and mechanism for producing zircon-hosted silica-rich MIs, as well as discussing implications for silicic volcanism and magmatism on the Moon.

## 2. Sample and Analytical Methods

The studied lunar breccia meteorite NWA 10049 was provided by Eric Twelker, who holds the main mass of this sample (Bouvier et al., 2017). Here, we give an overview of the petrology and geochemistry of this meteorite to provide context on the occurrence of the MI-bearing zircon (details for analytical methods and results are described in Text S1 and Tables S1–S3, in the supporting information, respectively). NWA 10049 is a feldspathic breccia mainly composed of a wide variety of feldspathic lithic clasts, glass fragments, and isolated mineral fragments (Figure S1). The lithic clasts mainly include anorthositic clasts, noritic/troctolitic anorthositic clasts, and impact-melt breccia clasts. Contrary to crystallized mafic impact melts, few basaltic clasts of unambiguous magmatic origin were observed in the studied section of NWA 10049. Bulk-rock composition measurements show that NWA 10049 has relatively high abundance of  $\text{Al}_2\text{O}_3$  (24.6 wt%) and low content of  $\text{FeO}$  (5.1 wt%), which were similar to lunar feldspathic meteorites (i.e.,  $\text{Al}_2\text{O}_3 > 25$  wt% and  $\text{FeO} < 7$  wt%; Figure S1). Unlike most feldspathic meteorites that have low bulk rock REE abundances, NWA 10049 exhibits moderately high concentrations of REE with a positive Eu-anomaly (Figure S1).

For the MI-bearing zircon fragment in NWA 10049, it was investigated using a variety of in situ analytical techniques. Back-scattered electron (BSE) images were collected by using a FEI Scios dual-beam focused ion beam/scanning electron microscope at the Institute of Geochemistry, Chinese Academy of Sciences. The operating conditions were 15–20 kV accelerating voltage, 1.6–3.2 nA beam current, and 7 mm working distance (Zeng et al., 2019). Cathodoluminescence (CL) image of zircon was collected using a Gatan MonoCL4 CL spectrometer attached to a JEOL JSM-7800F field emission scanning electron microscopy at the Institute of Geochemistry, Chinese Academy of Sciences. The operation conditions were 10 kV accelerating voltage and working distance of 14 mm. Raman spectra for zircon-1 were also collected (Text S2) and shown in Figure S2.

Major and minor elements (Table S4) of MIs in zircon were analyzed using a JEOL JXA 8230 electron microprobe at the Guilin University of Technology. The operation conditions were 15 kV accelerating voltage and 20 nA beam current with a focused beam of  $<1 \mu\text{m}$  (Zeng et al., 2018). Natural and synthetic standards were used, and matrix corrections were based on ZAF procedures. The typical detection limits for most elements are approximately 0.02–0.03 wt%.

Trace elements measurements (i.e., P, Ce, Sm, and Lu; Table S5) for MIs were carried out using CAMECA Nano-secondary ion mass spectrometry (Nano-SIMS) 50L at the Institute of Geology and Geophysics, Chinese Academy of Sciences. The grain mode analysis (see details in Hao et al., 2016) was used for the measurements. In this mode, a secondary ion image was first acquired by rastering a  $15 \times 15 \mu\text{m}$  area with a focused  $\sim 80 \text{ pA O}^-$  beam for  $\sim 2\text{--}3$  min. Then, based on the acquired secondary ion images, spot analyses

were carried out by deflecting the primary beam onto the selected areas (i.e.,  $2 \times 2 \mu\text{m}$ ) for  $\sim 5$  min each. A summary of analytical procedures was described in Text S3. Silicate glass standard (i.e., NIST 610; Table S6) was used to calibrate the trace element analyses using silicon as an internal elemental standard. The analytical precision at this scale varies from 2% to  $\sim 30\%$  (1 SD) depending on the concentration of the element.

U–Pb isotopic compositions of the studied zircon were measured using the same CAMECA Nano-SIMS 50L at the Institute of Geology and Geophysics, Chinese Academy of Sciences. The  $\text{O}_2^-$  primary beam was used, with a diameter of  $\sim 1.7 \mu\text{m}$  and a beam current of 500 pA. The Pb isotopic instrumental mass fractionation was less than 0.9% and thus negligible (Hu et al., 2019; Yang et al., 2012). A summary of analytical procedures was described in Text S4 (see also Yang et al., 2012). Zircon standards (i.e., M257 and AS3) were measured to assess the potential drift of the instrument during the analytical session. U–Pb dating results of the studied zircon and Pb isotopic data of zircon standards were provided in Tables S7 and S8, respectively. The Measured  $^{204}\text{Pb}/^{206}\text{Pb}$  ratios were used for the correction of common Pb (assumed by Stacey and Kramers 1975).

### 3. Characteristics of MI-bearing Zircon

#### 3.1. Occurrence and Internal Microstructures

The studied MI-bearing zircon (called “zircon-1”) was found in the matrix of lunar feldspathic breccia meteorite NWA 10049. This zircon shows irregular shape, with the grain size of  $\sim 200 \times 100 \mu\text{m}$ . From BSE and CL images (Figure 1), it is clear that zircon-1 is texturally and compositionally heterogeneous, having complex internal microstructures. These textures include (1) zoning-area. This texture was characterized by multiple, thin ( $< 1 \mu\text{m}$ ), concentric euhedral layers with different signal intensity in CL image (Figures 1c and 1d); (2) a fractured area that is bright in CL image (Figure 1a). The width and length of these fractures are 2 to  $5 \mu\text{m}$  and 10 to  $25 \mu\text{m}$ , respectively; (3) a smooth area, which is homogeneous in BSE image and appears dark in CL image (Figures 1a and 1c); (4) a granular recrystallized rim that distributed along the edges of the zircon, with a width of  $< 5 \mu\text{m}$  (Figures 1a and S3); and (5) MIs (i.e., MI-1, MI-2, and MI-3). These MIs show surrounded, irregular, or square shapes, with the size of  $\sim 3\text{--}5 \mu\text{m}$  (Figures 1e–1g).

#### 3.2. Geochemistry of MIs

MIs in zircon-1 are rhyolitic glass and exhibit relatively large compositional variation; they are predominately composed of  $\sim 78\text{--}92$  wt%  $\text{SiO}_2$ , with minor  $\sim 2\text{--}12$  wt%  $\text{Al}_2\text{O}_3$ , 0.3–1.2 wt%  $\text{K}_2\text{O}$ , and  $\sim 0.3\text{--}7$  wt%  $\text{Na}_2\text{O}$  (see Figure 2 and Table S4). The contents of  $\text{FeO}$ ,  $\text{TiO}_2$ ,  $\text{P}_2\text{O}_5$ , and  $\text{CaO}$  in these MIs are relative low (i.e.,  $<\sim 0.5$  wt%). In addition, the abundance of rare earth elements (i.e., Ce, Sm, and Lu) of these MIs is also variable (Table S5). REE concentration for MI-1 and MI-3 is generally within the compositional range for Apollo basalts, while MI-2 has relative lower abundance of REE (Figure 3). All of these MIs show LREE-depleted pattern, which is different from the REE patterns for Apollo mare basalts, high alkali suite, and KREEPy rocks (see Figure 3).

#### 3.3. U–Pb Isotopic Compositions and Ages

Twenty-two analyses were performed on the studied zircon-1 (Figures S4 and Table S7). This zircon has U and Th contents of 532 to 842 ppm and 125 to 198 ppm, respectively. The Th/U value varies from 0.265 to 0.296. U–Pb isotopic data for these points usually plots around the concordia curve with slight discordance (Figure 4a). For the concordant U–Pb data (Figure 4b), it is clear that the concordant  $^{207}\text{Pb}/^{206}\text{Pb}$  ages vary from  $4,312 \pm 17.7$  to  $4,382.3 \pm 39.9$  Ma (1 SD), potentially indicating a disturbance of the U–Pb system. The oldest concordant  $^{207}\text{Pb}/^{206}\text{Pb}$  age,  $4,382.3 \pm 39.9$  Ma, could be interpreted as the minimum age of the studied zircon-1.

### 4. Discussion

#### 4.1. Crystallization Age of Zircon-1

Multiple internal microstructures (e.g., brittle fractures and a granular recrystallized rim) that indicate complex history are observed in zircon-1 (Figure 1), suggesting that this zircon have experienced partial resetting or disturbance of the U–Pb system (Grange et al., 2013; Thiessen et al., 2018; Zhang et al., 2012). However, the error ellipses plot close to the concordia curve, suggesting that some part of the zircon have been either

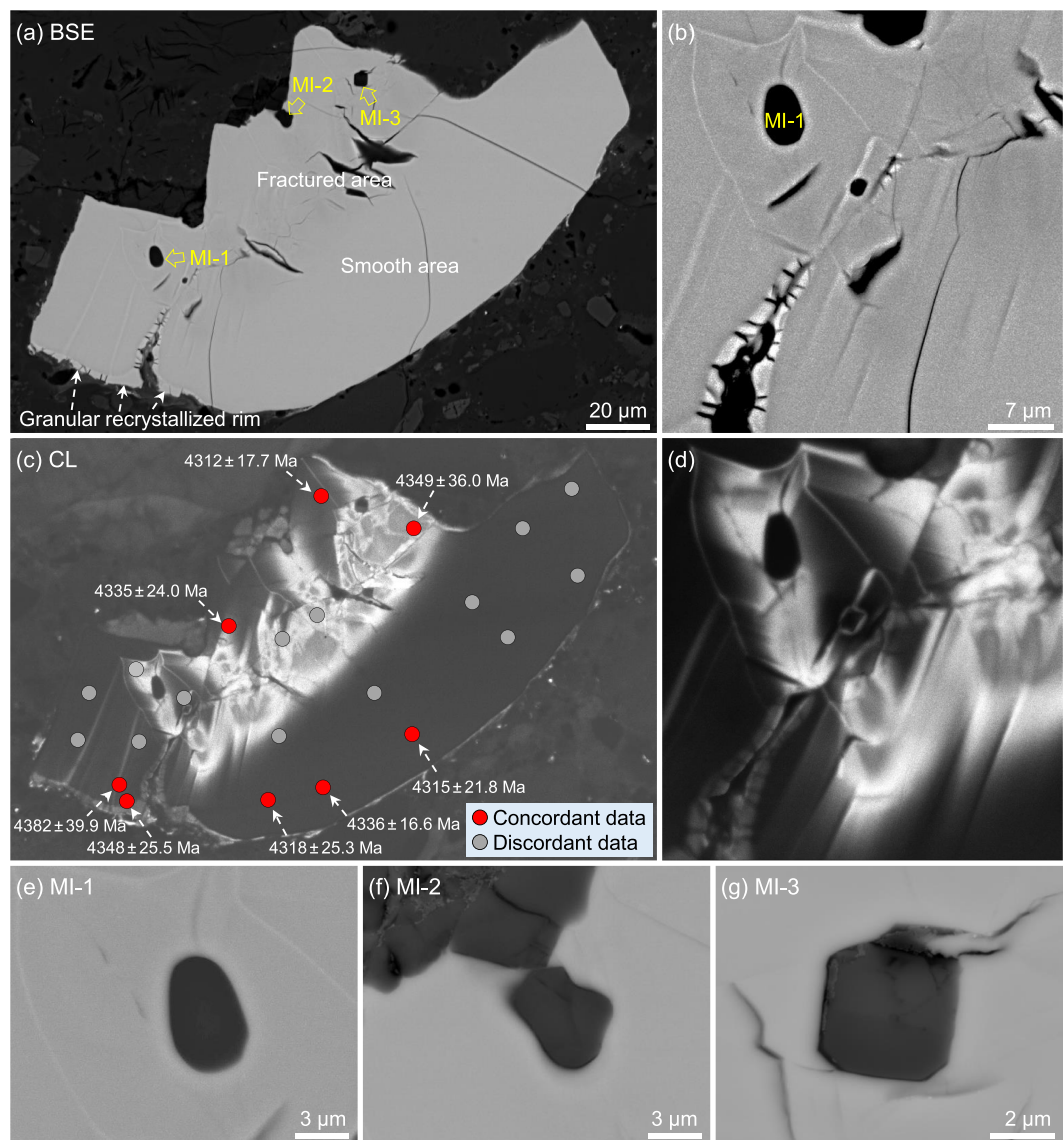


**Figure 1.** Microstructure of zircon-1 in NWA 10049. (a and b) Back-scattered electron (BSE) images showing complex internal structures, including zoning area, brittlely fractured area, smooth area, granular recrystallized rim, and melt inclusions (MIs). (c) Cathodoluminescence (CL) image with superimposed  $^{207}\text{Pb}/^{206}\text{Pb}$  ages for individual Nano-SIMS analysis. (d) A close-up image of CL image showing the detailed texture. (e–g) BSE images of individual melt inclusions denoted in (a).

completely recrystallized or unaffected by the disturbance. For a single zircon grain with a variety of concordant  $^{207}\text{Pb}/^{206}\text{Pb}$  ages, the oldest concordant  $^{207}\text{Pb}/^{206}\text{Pb}$  ages are usually interpreted as the minimum age of crystallization, while the relatively young ages would be explained as the reset age such as recrystallization event age (e.g., Bellucci et al., 2019; Grange et al., 2013; Nemchin et al., 2009). In the case of zircon-1 in NWA 10049, we therefore interpret that the oldest concordant  $^{207}\text{Pb}/^{206}\text{Pb}$  ages (i.e.,  $4,382 \pm 40$  Ma; Figure 4b) as the minimum age of crystallization.

#### 4.2. Mechanism for Producing Silica-rich MI in Zircon-1: Silicate Liquid Immiscibility

The chemical characteristics of zircon-hosted MIs preserve clues about their formation mechanism (e.g., Chupin et al., 1998). For silica-rich MIs in zircon-1, they compositionally show (1) relatively high abundance of  $\text{SiO}_2$ ,  $\text{Al}_2\text{O}_3$ ,  $\text{K}_2\text{O}$ , and  $\text{Na}_2\text{O}$ ; (2) relatively low concentrations of  $\text{FeO}$ ,  $\text{MgO}$ ,  $\text{CaO}$ ,  $\text{TiO}_2$ , and  $\text{P}_2\text{O}_5$ ; and (3) low abundance of REE, with LREE-depleted pattern (Figures 2 and S5). Compared with the bulk

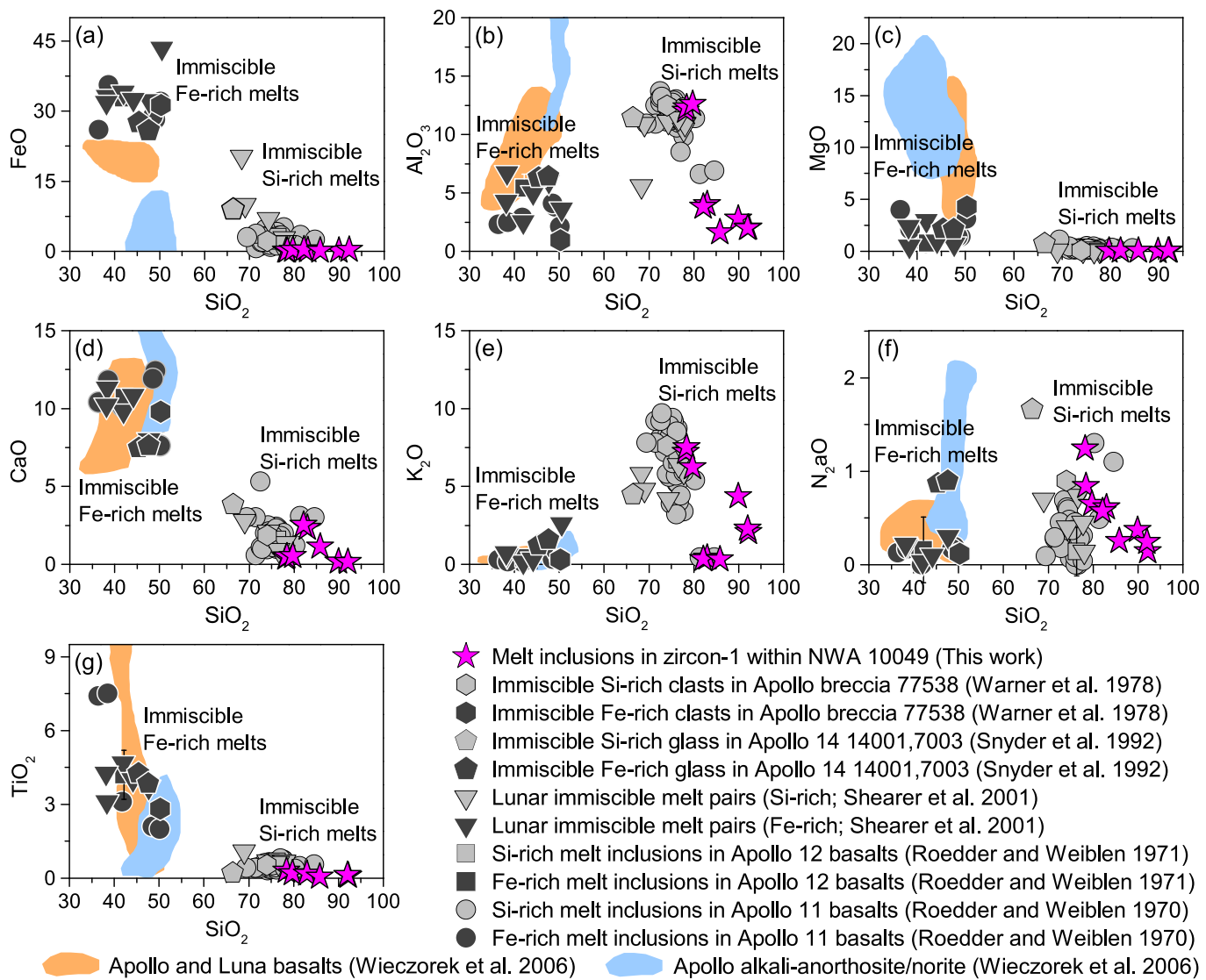


**Figure 2.** Chemical composition of melt inclusions in zircon-1, compared with the composition of immiscible Si-rich and Fe-rich clasts in Apollo breccia 77538 (Warner et al., 1978), lunar immiscible melt pairs (Shearer et al., 2001), and Si-rich and Fe-rich inclusions in Apollo 11/12/14 rocks (Roedder & Weiben, 1970; Roedder & Weiben, 1971; Snyder et al., 1993). The composition of Apollo/Luna basalts and alkali-anorthosite/norite is also plotted for comparison (table A3.3 and table A3.11 of Wieczorek et al., 2006).

composition of Apollo-evolved alkali suite (i.e.,  $\text{SiO}_2 < \sim 55$  wt%,  $\text{MgO} = \sim 0.2\text{--}15$  wt%,  $\text{CaO} = 8\text{--}20$  wt%, and  $\text{K}_2\text{O} < 2$  wt%; Snyder et al., 1995; table 5.34 of Papike et al., 1998), silica-rich MIs within zircon-1 show key chemical differences (i.e.,  $\text{SiO}_2 = \sim 80\text{--}90$  wt%,  $\text{MgO} < 0.05$  wt%,  $\text{CaO} < \sim 3$  wt%, and  $\text{K}_2\text{O} = 0.3\text{--}7$  wt%; see Figure 2). This indicates that zircon-1 was not like crystallized from lunar-evolved alkali melt.

On the Moon, the evolved silica-rich melts can be produced by crustal partial melting and extreme fractional crystallization (Gullikson et al., 2016; Jolliff et al., 1999). In general, silicic melts produced from crustal partial melting and extreme fractional crystallization processes would be expected to be rich in Ti, P, and incompatible trace elements (Taylor et al., 1980). In addition, a HREE-depleted pattern is also an evidence for crustal partial melting or an extreme fractional crystallization process (Warner et al., 1978). However, these chemical features are not consistent with the chemistry of the zircon-hosted MIs: They instead show relatively low concentrations of ITEs (Ti, P, and REE) and exhibit LREE-depleted pattern (Figures 2 and 3). We, therefore, suggest that zircon-1 did not likely crystallize from the silica-rich melt produced from crustal partial melting and extreme fractional crystallization processes.

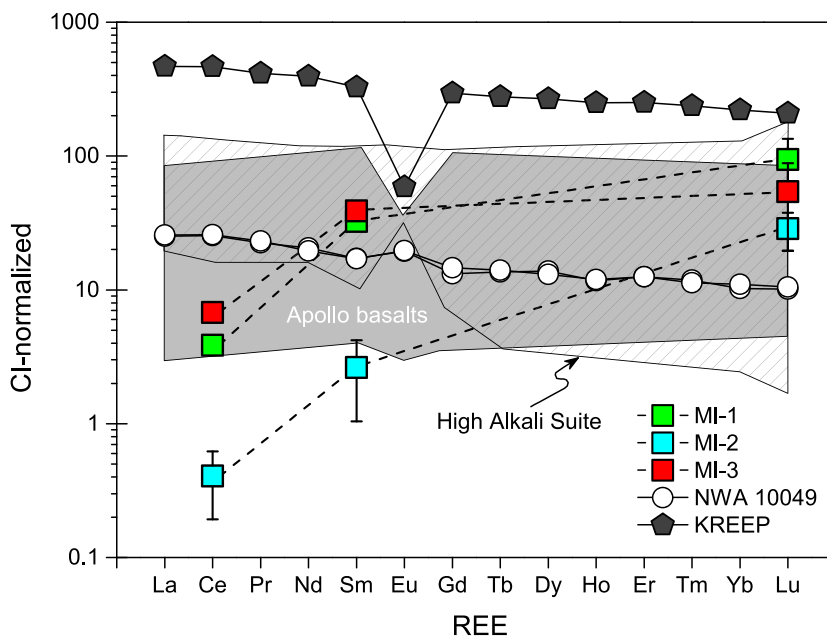


**Figure 3.** CI-chondrite normalized REE patterns for the studied melt inclusions, compared with the REE abundance of NWA 10049, bulk rock Apollo mare basalts (dark gray area; Papike et al., 1998), bulk rock Apollo alkali suite samples (Light grey network area; Wieczorek et al., 2006), and high-K KREEP (Warren, 1989). Error bar reflects 1 $\sigma$  standard deviation variations.

Another mechanism that could produce lunar silicic melt is silicate liquid immiscibility (Roedder & Weiben, 1970; Taylor et al., 1980). It is a process that occurs when extensive crystal fractionation (90–98%) of a basaltic magma takes place, at which point the residual melt exsolves into Si-(K)-rich and Fe-rich melt (Hess, 1989; Roedder, 1984). Previous studies have provided empirical and theoretical chemical criteria for identifying silicate liquid immiscibility (e.g., Taylor et al., 1980). These criteria include the following: (1) In general, elements with high charge densities (e.g., Fe, Mg, Ca, Ti, and P) tend to concentrate in Fe-rich melts, while elements with low charge densities (e.g., Si, Al, K, Na, Rb, and Cs) tend to reside in the Si-rich melt (e.g., Hess & Rutherford, 1974). For the studied MIs in zircon-1, they contain high content of SiO<sub>2</sub>, Al<sub>2</sub>O<sub>3</sub>, K<sub>2</sub>O, and Na<sub>2</sub>O and lower concentrations of FeO, MgO, CaO, TiO<sub>2</sub>, and P<sub>2</sub>O<sub>5</sub> (Figure 2). Such

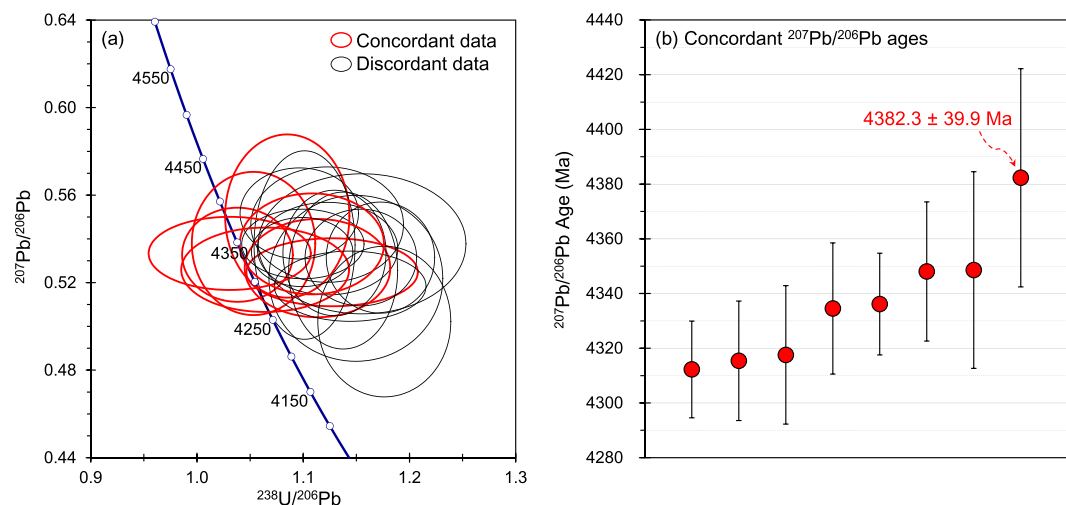


**Figure 4.** (a) U-Pb data for zircon-1 from breccia meteorite NWA 10049. Read ellipses represent the concordant U-Pb isotope data, while black ellipses represent the discordant U-Pb isotope data. Data-point error ellipses are 2 $\sigma$ . (b) Concordant  $^{207}\text{Pb}/^{206}\text{Pb}$  ages. Error bars for  $^{207}\text{Pb}/^{206}\text{Pb}$  ages are 1 $\sigma$ .

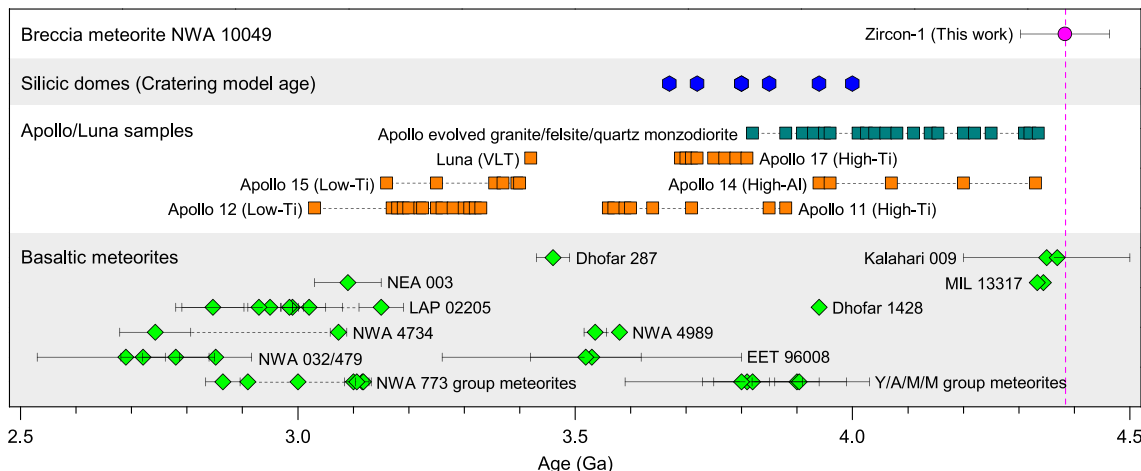


**Figure 5.** Crystallization age ( $4.382 \pm 0.08$  Ga;  $2\sigma$ ) of zircon-1 in NWA 10049, compared with the ages of Apollo-evolved rocks from the alkali suite (i.e., granite/felsite/quartz monzodiorite; Wieczorek et al., 2006 and references therein), Apollo/Luna basalts (adapted from Joy & Arai, 2013), and lunar basaltic meteorites (Curran et al., 2019 and references therein; Joy & Arai, 2013; Shaulis et al., 2013; Snape et al., 2018; Wu & Hsu, 2020; Xue et al., 2019). The cratering model ages of lunar silicic domes are also plotted for comparison (Ashley et al., 2016; Shirley et al., 2016; Wagner et al., 2002, 2010).

chemical characteristics are precisely as expected for a silica-rich immiscible melts. (2) Evidence for liquid immiscibility on the Moon has been documented in MIs in minerals and mesostasis in Apollo mare basalts (e.g., high-Ti basalt 10071, low-Ti ilmenite basalt 10050, and olivine basalt 12018; Roedder et al., 1970, 1971; Roedder, 1984) as well as breccia sample 77538 (Warner et al., 1978). These reported immiscible silica-rich melts show similar geochemical characteristics to our studied zircon-hosted MIs (Figure 2). (3) Taylor et al. (1980) suggested that bulk  $K_2O/P_2O_5$  ratios is a useful indicator to distinguish immiscible high-Si melt ( $K_2O/P_2O_5 > 4$ ) and immiscible high-Fe melt ( $K_2O/P_2O_5 < 0.4$ ). The studied MIs in zircon-1 have  $K_2O/P_2O_5$  ratios of  $> 23$  (Table S4), consistent with the expected lunar immiscible silica-rich melt element ratios. (4) When silicate liquid immiscibility took place, REEs likely preferentially concentrated into the Fe-rich melt, resulting in the depletion of REE in the companion Si-rich melt (e.g., Shearer et al., 2001; Veksler et al., 2007). The relatively low abundance of REE in MIs of zircon-1 is in agreement with the chemical characteristics of immiscible Si-rich melts.

#### 4.3. Implications for Silicate Liquid Immiscibility and Silicic Volcanism on the Moon

Lunar meteorites are random samples probably ejected far from Apollo and Luna landing sites (Korotev et al., 2009); this indicates that our studied MI-bearing zircon in NWA 10049 provides supplementary evidence for documenting immiscible silica-rich melts on the Moon. Unlike the small (i.e.,  $< 20 \mu m$  in size) irregular lunar zircon in impact-generated rocks formed at a fast cooling rate (e.g., Grange et al., 2011; Norman & Nemchin, 2014), zircon-1 has relatively large grain size of  $\sim 200 \mu m$  (Figure 1). This suggests that the cooling rate for immiscible silica-rich melts where zircon-1 crystallized from would be relatively slow (more suggestive of a plutonic environment than a surface process). This is consistent with previous investigation by Neal and Taylor (1989) that the cooling rates of basaltic magma ought to be relatively slow (in a plutonic or deep hypabyssal setting) in order to allow separation of immiscible liquid into a Fe-rich and Si-rich chemical fractions.

The pulse of magmatism recorded by lunar-evolved granites/felsite/quartz monzodiorite samples at  $\sim 3.88$  to  $4.33$  Ga (Grange et al., 2009; Meyer et al., 1996; Thiessen et al., 2018) is somewhat younger than the timing of the most ancient lunar basaltic volcanism ( $\sim 4.37$  Ga) recorded in lunar meteorites (Curran et al., 2019; Snape et al., 2018; Terada et al., 2007) and the  $\sim 4.382$  Ga zircon-1 clast presented here (Figure 5). Investigation of Apollo samples and remote-sensing data has shown that the evolved silica-rich material is present at some of the Apollo landing sites and has been seen outcropping at volcanic complexes across the Moon (Bruno et al., 1991; Glotch et al., 2010; Hagerty et al., 2006; Hawke et al., 2003; Head & McCord, 1978; Jolliff et al., 2011). Notably, lunar silicic volcanic occurrences (e.g., Hansteen Alpha, Gruithuisen domes, Helmet, Compton-Belkovich, and Lassell Massif) were found to range in age from Late Imbrian to Pre-Nectarian (i.e.,

cratering model ages of ~3.67–4.0 Ga; Ashley et al., 2016; Shirley et al., 2016; Wagner et al., 2002, 2010), younger than the age of silica-rich melts recorded by ~4.382 Ga zircon-1 in NWA 10049 (Figure 5). Whether large-scale segregation and eruption of silica-rich fraction of immiscible melts are debatable (Charlier et al., 2011; Hagerty et al., 2006), but the ranges of ages (i.e., from ~3.67 to 4.38 Ga) for lunar siliceous volcanic fields and silica-rich melts in zircon-1 imply that silicate liquid immiscibility was a prolonged process in the evolution of lunar magmatism.

## 5. Conclusions

For the studied zircon-1 in lunar breccia NWA 10049, it contains Si-rich MIs that are compositionally similar with immiscible silica-rich melts reported in Apollo rocks. This zircon was most likely crystallized from an immiscible silica-rich melts on the Moon. Nano-SIMS measurements of zircon-1 show a wide range of  $^{207}\text{Pb}/^{206}\text{Pb}$  ages, indicating that this zircon has been partially reset by post-crystallization processes. We interpret that the oldest concordant  $^{207}\text{Pb}/^{206}\text{Pb}$  ages (i.e.,  $4.382 \pm 0.08$  Ga;  $2\sigma$ ) as the minimum age of crystallization. This age is older than the ages for Apollo-returned granites (up to 4.33 Ga) and ancient basaltic volcanism (i.e., up to ~4.37 Ga), making our studied zircon the oldest microscale evidence for documenting lunar silicate liquid immiscibility.

Considering the young silicic volcanism (with a Late Imbrian cratering model ages of ~3.67 Ga) that has been detected on the Moon, the identification of ~4.38 Ga (Pre-Nectarian ages) ancient silica-rich melts recorded by zircon-1 reveals that there would be a prolonged silicic magmatism occurred on the Moon than previously thought. To test this hypotheses, more chronology works on lunar-evolved granite/felsite samples (e.g., evolved clasts within meteorites) would be necessary in the future. In 2020, rocks derived from silica-rich lunar volcanism may be sampled by Chinese Chang'e-5 mission, which aims to sample and return to Earth regolith from the Rümker region. Located close to the proposed landing sites is a small topographic mound called “East Dome” ( $49.85^\circ\text{W}, 43.68^\circ\text{N}$ ; Qian et al., 2018), thought to be an expression of low-Th extrusive siliceous volcanism (Glotch et al., 2010) in the Imbrian Period (Head & McCord, 1978). Although younger (Imbrian age rather than Pre-Nectarian ages), sampling of this evolved volcanic field will have important implications for understanding silicic volcanism on the Moon through time.

## Acknowledgments

The authors would like to thank Ziyuan Ouyang, Yun Liu, Dan Zhu, Aicheng Zhang, Wei Yang, and Guiqin Wang for their comments and suggestions about this work. X. Zeng would also like to thank Yizhi Liu and Yan Zhong for their help during the electron microprobe measurements at the Guilin University of Technology. We also thank Dr. Merle and an anonymous reviewer for their helpful comments, as well as Dr. Andrew J. Dombard for his editorial handling. This study was supported by the National Natural Science Foundation of China (Nos. 41941003 and 41931077), opening fund of Key Laboratory of Earth and Planetary Physics (No. DQXX201701), STFC (ST/M001253/1), B-type Strategic Priority Program of the Chinese Academy of Sciences (No. XDB41000000), China Postdoctoral Science Foundation to X. Zeng, and Royal Society (RS/UF140190) grants to K. Joy. The geochemistry data used in this manuscript are available online (<https://doi.org/10.6084/m9.figshare.11590311.v1>).

## References

- Ashley, J. W., Robinson, M. S., Stopar, J. D., Glotch, T. D., Hawke, B. R., Van der Bogert, C. H., et al. (2016). The Lassell massif—A silicic lunar volcano. *Icarus*, 273, 248–261. <https://doi.org/10.1016/j.icarus.2015.12.036>
- Bellucci, J. J., Nemchin, A. A., Grange, M., Robinson, K. L., Collins, G., Whitehouse, M. J., & Kring, D. A. (2019). Terrestrial-like zircon in a clast from an Apollo 14 breccia. *Earth and Planetary Science Letters*, 510, 173–185.
- Bouvier, A., Gattaceca, J., Agee, C., Grossman, J., & Metzler, K. (2017). The meteoritical bulletin, no. 104. *Meteoritics & Planetary Science*, 52(10), 2284–2284.
- Bruno, B. C., Lucey, P. G., & Hawke, B. R. (1991). High resolution UV visible spectroscopy of lunar red spots, Proc. Lunar Planet. Sci. Conf. 21st, 405–415.
- Charlier, B., & Grove, T. L. (2012). Experiments on liquid immiscibility along tholeiitic liquid lines of descent. *Contributions to Mineralogy and Petrology*, 164(1), 27–44.
- Charlier, B., Namur, O., Toplis, M. J., Schiano, P., Cluzel, N., Higgins, M. D., & Auwera, J. V. (2011). Large-scale silicate liquid immiscibility during differentiation of tholeiitic basalt to granite and the origin of the Daly gap. *Geology*, 39(10), 907–910.
- Chupin, S. V., Chupin, V. P., Barton, J. M., & Barton, E. S. (1998). Archean melt inclusions in zircon from quartzite and granitic orthogneiss from South Africa; magma compositions and probable sources of protoliths. *European Journal of Mineralogy*, 10(6), 1241–1251.
- Curran, N. M., Joy, K. H., Snape, J. F., Pernet-Fisher, J. F., Gilmour, J. D., Nemchin, A. A., et al. (2019). The early geological history of the Moon inferred from ancient lunar meteorite Miller Range 13317. *Meteoritics and Planetary Science*, 54(7), 1401–1430. <https://doi.org/10.1111/maps.13295>
- Fagan, T. J., Kashima, D., Wakabayashi, Y., & Sugino-hara, A. (2014). Case study of magmatic differentiation trends on the Moon based on lunar meteorite Northwest Africa 773 and comparison with Apollo 15 quartz monzodiorite. *Geochimica et Cosmochimica Acta*, 133, 97–127.
- Grange, M. L., Nemchin, A. A., Pidgeon, R. T., Timms, N., Muhling, J. R., & Kennedy, A. K. (2009). Thermal history recorded by the Apollo 17 impact melt breccia 73217. *Geochimica et Cosmochimica Acta*, 73(10), 3093–3107.
- Glotch, T. D., Lucey, P. G., Bandfield, J. L., Greenhagen, B. T., Thomas, I. R., Elphic, R. C., et al. (2010). Highly silicic compositions on the Moon. *Science*, 329(5998), 1510–1513. <https://doi.org/10.1126/science.1192148>
- Grange, M. L., Nemchin, A. A., Timms, N., Pidgeon, R. T., & Meyer, C. (2011). Complex magmatic and impact history prior to 4.1 Ga recorded in zircon from Apollo 17 South Massif aphanitic breccia 73235. *Geochimica et Cosmochimica Acta*, 75(8), 2213–2232.
- Grange, M. L., Pidgeon, R. T., Nemchin, A. A., Timms, N. E., & Meyer, C. (2013). Interpreting U-Pb data from primary and secondary features in lunar zircon. *Geochimica et Cosmochimica Acta*, 101, 112–132.
- Gullikson, A. L., Hagerty, J. J., Reid, M. R., Rapp, J. F., & Draper, D. S. (2016). Silicic lunar volcanism: Testing the crustal melting model. *American Mineralogist*, 101(10), 2312–2321.

- Hagerty, J. J., Lawrence, D. J., Hawke, B. R., Vaniman, D. T., Elphic, R. C., & Feldman, W. C. (2006). Refined thorium abundances for lunar red spots: Implications for evolved, nonmare volcanism on the Moon. *Journal of Geophysical Research*, 111, E06002. <https://doi.org/10.1029/2005JE002592>
- Hao, J. L., Yang, W., Luo, Y., Hu, S., Yin, Q. Z., & Lin, Y. T. (2016). NanoSIMS measurements of trace elements at the micron scale interface between zircon and silicate glass. *Journal of Analytical Atomic Spectrometry*, 31(12), 2399–2409.
- Hawke, B. R., Lawrence, D. J., Blewett, D. T., Lucey, P. G., Smith, G. A., Spudis, P. D., & Taylor, G. J. (2003). Hansteen Alpha: A volcanic construct in the lunar highlands. *Journal of Geophysical Research*, 108(E7), 5069. <https://doi.org/10.1029/2002JE002013>
- Head, J. W., & McCord, T. B. (1978). Imbrian-age highland volcanism on the Moon: The Gruithuisen and Mairan domes. *Science*, 199(4336), 1433–1436. <https://doi.org/10.1126/science.199.4336.1433>
- Hess, P. C. (1989). Highly evolved liquids from the fractionation of mare and nonmare basalts, paper presented at Workshop on the Moon in Transition, LPI Tech Report 89-03. Lunar and Planetary Institute, Houston, Texas.
- Hess, P. C., & Rutherford, M. J. (1974). Element fractionation between immiscible melts. *Lunar Science V*, 328–330.
- Hinton, R. W., & Meyer, C. (1991). Ion probe analysis of zircon and ytterobetafite in a lunar granite. *Tehnicki Vjesnik*, 18(4), 485–495.
- Hu, S., Lin, Y., Zhang, J., Hao, J., Xing, W., Zhang, T., et al. (2019). Ancient geologic events on Mars revealed by zircons and apatites from the Martian regolith breccia NWA 7034. *Meteoritics & Planetary Science*, 54(4), 850–879. <https://doi.org/10.1111/maps.13256>
- Jakobsen, J. K., Veksler, I. V., Tegner, C., & Brooks, C. K. (2005). Immiscible iron- and silica-rich melts in basalt petrogenesis documented in the Skærgaard intrusion. *Geology*, 33, 885–888.
- Jolliff, B. L. (1991). Fragments of quartz monzodiorite and felsite in Apollo 14 soil particles. Proceedings of the 21st Lunar and Planetary Science Conference, 101–118.
- Jolliff, B. L., Floss, C., McCallum, I. S., & Schwartz, J. M. (1999). Geochemistry, petrology, and cooling history of 14161, 7373: A plutonic lunar sample with textural evidence of granitic-fraction separation by silicate-liquid immiscibility. *American Mineralogist*, 84(5-6), 821–837.
- Jolliff, B. L., Wiseman, S. A., Lawrence, S. J., Tran, T. N., Robinson, M. S., Sato, H., et al. (2011). Non-mare silicic volcanism on the lunar farside at Compton–Belkovich. *Nature Geoscience*, 4(8), 566–571. <https://doi.org/10.1038/ngeo1212>
- Joy, K. H., & Arai, T. (2013). Lunar meteorites: New insights into the geological history of the Moon. *Astronomy & Geophysics*, 54(4), 4–28.
- Joy, K. H., Burgess, R., Hinton, R., Fernandes, V. A., Crawford, I. A., Kearsley, A. T., Irving, A. J. (2011). Petrogenesis and chronology of lunar meteorite Northwest Africa 4472: A KREEPy regolith breccia from the Moon. *Geochimica et Cosmochimica Acta*, 75(9), 2420–2452.
- Korotev, R. L., Zeigler, R. A., Jolliff, B. L., Irving, A. J., & Bunch, T. E. (2009). Compositional and lithological diversity among brecciated lunar meteorites of intermediate iron concentration. *Meteoritics & Planetary Science*, 44, 1287–1322.
- Lin, Y., Shen, W., Liu, Y., Xu, L., Hofmann, B. A., Mao, Q., et al. (2012). Very high-K KREEP-rich clasts in the impact melt breccia of the lunar meteorite SaU 169: New constraints on the last residue of the lunar magma ocean. *Geochimica et Cosmochimica Acta*, 85, 19–40. <https://doi.org/10.1016/j.gca.2012.02.011>
- Mattinson, J. M., Graubard, C. M., Parkinson, D. L., & McLelland, W. C. (1996). U–Pb reverse discordance in zircons: the role of fine-scale oscillatory zoning and sub-microscopic transport of Pb. *Geophys. Monogr.*, (Vol. 95, pp. 355–370). Washington, D. C: American Geophysical Union.
- Merle, R. E., Nemchin, A. A., Whitehouse, M. J., Pidgeon, R. T., Grange, M. L., Snape, J. F., & Thiessen, F. (2017). Origin and transportation history of lunar breccia 14311. *Meteoritics & Planetary Science*, 52(5), 842–858.
- Meyer, C., Williams, I. S., & Compston, W. (1996). Uranium-lead ages for lunar zircons: Evidence for a prolonged period of granophyre formation from 4.32 to 3.88 Ga. *Meteoritics & Planetary Science*, 31(3), 370–387.
- Neal, C. R., & Taylor, L. A. (1989). The nature and barium partitioning between immiscible melts—A comparison of experimental and natural systems with reference to lunar granite petrogenesis. In Lunar and Planetary Science Conference Proceedings (Vol. 19, pp. 209–218).
- Nemchin, A., Timms, N., Pidgeon, R., Geisler, T., Reddy, S., & Meyer, C. (2009). Timing of crystallization of the lunar magma ocean constrained by the oldest zircon. *Nature Geoscience*, 2(2), 133.
- Nemchin, A. A., Grange, M. L., Pidgeon, R. T., & Meyer, C. (2012). Lunar zirconology. *Australian Journal of Earth Sciences*, 59(2), 277–290.
- Norman, M. D., & Nemchin, A. A. (2014). A 4.2 billion year old impact basin on the Moon: U–Pb dating of zirconolite and apatite in lunar melt rock 67955. *Earth and Planetary Science Letters*, 388, 387–398.
- Papike, J. J., Ryder, G., & Shearer, C. K. (1998). Lunar samples. In J. Papike (Ed.), *Planetary materials, J. Reviews in Mineralogy*, (Vol. 36, pp. 5.1–5.234). Washington, D.C: Mineralogical Society of America.
- Qian, Y. Q., Xiao, L., Zhao, S. Y., Zhao, J. N., Huang, J., Flahaut, J., et al. (2018). Geology and Scientific Significance of the Rümker Region in Northern Oceanus Procellarum: China's Chang'E-5 Landing Region. *Journal of Geophysical Research, Planets*, 123(6), 1407–1430. <https://doi.org/10.1029/2018JE005595>
- Roedder, E. (1979). Silicate liquid immiscibility in magmas. In H. S. Yoder, Jr. (Ed.), *The Evolution of Igneous Rocks. Fiftieth Anniversary Perspectives*, (pp. 15–58). Princeton, NJ: Princeton University Press.
- Roedder, E. (1984). *Fluid Inclusions, Reviews in Mineralogy*, (Vol. 12). Washington, D.C: Mineralogical Society of America.
- Roedder, E., & Weible, P. W. (1970). Lunar petrology of silicate melt inclusions, Apollo 11 rocks. *Geochimica et Cosmochimica Acta*. Supplement, 1, 801.
- Roedder, E., & Weible, P. W. (1971). Petrology of silicate melt inclusions, Apollo 11 and Apollo 12 and terrestrial equivalents. Proceedings of the 2nd Lunar Science Conference, 507–528.
- Rutherford, M. J., Hess, P. C., Ryerson, F. J., Campbell, H. W., & Dick, P. A. (1976). The chemistry, origin and petrogenetic implications of lunar granite and monzonite. In Lunar and Planetary Science Conference Proceedings (Vol. 7, pp. 1723–1740).
- Seddio, S. M., Jolliff, B. L., Korotev, R. L., & Zeigler, R. A. (2013). Petrology and geochemistry of lunar granite 12032, 366-19 and implications for lunar granite petrogenesis. *American Mineralogist*, 98(10), 1697–1713.
- Shaulis, B. J., Righter, M., Lapen, T. J., & Irving, A. J. (2013). 3.1 Ga crystallization age of magnesian and ferroan gabbro lithologies in lunar meteorites Northwest Africa 773, 3170, 6950 and 7007 and evidence for 3.95 Ga components in NWA 773 polymict breccia. In Lunar and Planetary Science Conference (Vol. 44, p. 1781).
- Shearer, C. K., Papike, J. J., & Spilde, M. N. (2001). Trace-element partitioning between immiscible lunar melts: An example from naturally occurring lunar melt inclusions. *American Mineralogist*, 86(3), 238–246.
- Shirley, K. A., Zanetti, M., Jolliff, B. V., van der Bogert, C. H., & Hiesinger, H. (2016). Crater size-frequency distribution measurements and age of the Compton–Belkovich volcanic complex. *Icarus*, 273, 214–223.
- Snape, J. F., Curran, N. M., Whitehouse, M. J., Nemchin, A. A., Joy, K. H., Hopkinson, T., et al. (2018). Ancient volcanism on the Moon: Insights from Pb isotopes in the MIL 13317 and Kalahari 009 lunar meteorites. *Earth and Planetary Science Letters*, 502, 84–95.

- Snyder, G. A., Taylor, L. A., & Crozaz, G. (1993). Rare earth element selenochemistry of immiscible liquids and zircon at apollo 14: An ion probe study of evolved rocks on the moon. *Geochimica et Cosmochimica Acta*, 57(5), 1143–1149.
- Snyder, G. A., Taylor, L. A., & Halliday, A. N. (1995). Chronology and petrogenesis of the lunar highlands alkali suite: Cumulates from KREEP basalt crystallization. *Geochimica et Cosmochimica Acta*, 59(6), 1185–1203.
- Stacey, J. T., & Kramers, J. D. (1975). Approximation of terrestrial lead isotope evolution by a two-stage model. *Earth and Planetary Science Letters*, 26(2), 207–221.
- Taylor, G. J., Warner, R. D., Keil, K., Ma, M. S., & Schmitt, R. A. (1980). Silicate liquid immiscibility, evolved lunar rocks and the formation of KREEP. In *Lunar Highlands Crust* (pp. 339–352).
- Terada, K., Anand, M., Sokol, A. K., Bischoff, A., & Sano, Y. (2007). Cryptomare magmatism 4.35 Gyr ago recorded in lunar meteorite Kalahari 009. *Nature*, 450(7171), 849–852.
- Thiessen, F., Nemchin, A. A., Snape, J. F., Bellucci, J. J., & Whitehouse, M. J. (2018). Apollo 12 breccia 12013: Impact-induced partial Pb loss in zircon and its implications for lunar geochronology. *Geochimica et Cosmochimica Acta*, 230, 94–111.
- Thomas, J. B., Bodnar, R. J., Shimizu, N., & Chesner, C. A. (2003). Melt inclusions in zircon. *Reviews in Mineralogy and Geochemistry*, 53(1), 63–87.
- Veksler, I. V., Dorfman, A. M., Borisov, A. A., Wirth, R., & Dingwell, D. B. (2007). Liquid immiscibility and the evolution of basaltic magma. *Journal of Petrology*, 48(11), 2187–2210.
- Wagner, R., Head III, J. W., Wolf, U., & Neukum, G. (2002). Stratigraphic sequence and ages of volcanic units in the Gruithuisen region of the Moon. *Journal of Geophysical Research, Planets*, 107(E11), 5104. <https://doi.org/10.1029/2002JE001844>
- Wagner, R., Head, J. W. III, Wolf, U., & Neukum, G. (2010). Lunar red spots: Stratigraphic sequence and ages of domes and plains in the Hansteen and Helmet regions on the lunar nearside. *Journal of Geophysical Research*, 115(E6), E06015. <https://doi.org/10.1029/2009JE003359>
- Warner, R. D., Taylor, G. J., Mansker, W. L., & Keil, K. L. A. U. S. (1978). Clast assemblages of possible deep-seated/77517/and immiscible-melt/77538/origins in Apollo 17 breccias. In *Lunar and Planetary Science Conference Proceedings* (Vol. 9, pp. 941–958).
- Warren, P. H. (1989). KREEP: Major-element diversity, traceelement uniformity (almost). In G. J. Taylor, & P. H. Warren (Eds.), *LPI Technical Report/Workshop on Moon in transition: Apollo 14, KREEP, and evolved lunar rocks*, (Vol. 89-03, pp. 149–153). Lunar and Planetary Institute: Houston, Texas.
- Wieczorek, M. A., Jolliff, B. L., Khan, A., Pritchard, M. E., Weiss, B. P., Williams, J. G., et al. (2006). The constitution and structure of the lunar interior. *Reviews in Mineralogy and Geochemistry*, 60(1), 221–364. <https://doi.org/10.2138/rmg.2006.60.3>
- Wu, Y., & Hsu, W. (2020). Mineral chemistry and in situ UPb geochronology of the mare basalt Northwest Africa 10597: Implications for low-Ti mare volcanism around 3.0 Ga. *Icarus*, 338, 113531.
- Xue, Z., Xiao, L., Neal, C. R., & Xu, Y. (2019). Oldest high-Ti basalt and magnesian crustal materials in feldspathic lunar meteorite Dhofar 1428. *Geochimica et Cosmochimica Acta*, 266, 74–108. <https://doi.org/10.1016/j.gca.2019.06.022>
- Yang, W., Lin, Y. T., Zhang, J. C., Hao, J. L., Shen, W. J., & Hu, S. (2012). Precise micrometre-sized Pb-Pb and U-Pb dating with NanoSIMS. *Journal of Analytical Atomic Spectrometry*, 27(3), 479–487.
- Zeng, X., Joy, K. H., Li, S., Pernet-Fisher, J. F., Li, X., Martin, D. J. P., et al. (2018). Multiple lithic clasts in lunar breccia Northwest Africa 7948 and implication for the lithologic components of lunar crust. *Meteoritics & Planetary Science*, 53(5), 1030–1050. <https://doi.org/10.1111/maps.13049>
- Zeng, X., Shang, Y., Li, S., Li, X., Wang, S., & Li, Y. (2019). The layered structure model for winonaite parent asteroid implicated by textural and mineralogical diversity. *Earth, Planets and Space*, 71(1), 38.
- Zhang, A. C., Taylor, L. A., Wang, R. C., Li, Q. L., Li, X. H., Patchen, A. D., & Liu, Y. (2012). Thermal history of Apollo 12 granite and KREEP-rich rock: Clues from Pb/Pb ages of zircon in lunar breccia 12013. *Geochimica et Cosmochimica Acta*, 95, 1–14.